

PROPOSAL AND VERIFICATION OF RIP CURRENT DETECTION USING AI

T. Ishikawa¹, R. Shimada², R. Sawagashira² and T. Komine²

¹Research and Development Initiative, Chuo University, 1-13-27, Kasuga Bunkyo-ku, Tokyo 112-8551, Japan. ishikawa.195@g.chuo-u.ac.jp.

²Faculty of Science and Engineering, Chuo University, 1-13-27, Kasuga Bunkyo-ku, Tokyo 112-8551, Japan.

1. Introduction

There are from 2,000 to 3,000 rescues including those of unconscious people every year on the beaches of Japan, as shown in Fig. 1. The occurrence of drowning accidents is mainly caused by the rip current (Ishikawa et al., 2014), it accounts for 48 % of drowning accidents, as shown in Fig. 2. Also, in Australia, the United States and the United Kingdom, more than 50 % of rescue accidents are caused by rip currents (Brighton et al., 2013). In order to reduce the rip current accidents, beach users need to recognize rip currents, then they have to avoid them using risk assessment. However, it is the difficulty of risk recognition and judgement under the momentary change in natural phenomenon for beach users. Especially, almost all beach users understand the risk in the case of high wave conditions due to easy visual understanding, whereas they cannot understand rip currents the same way. On the other hand, swimming areas along the shore are very limited, however the number of lifeguards is small at around 1 lifeguard compared to the thousands of beach users. In addition, beach users sometimes enter unpatrolled areas outside the swimming areas. Therefore, we developed a new technology that can automatically detect the rip currents by the Artificial Intelligence (AI), and notify beach users and lifeguards using the Internet of Things (IoT). In this study, we verified the accuracy of the rip current detection by the AI, using a field measurement, an image analysis and a numerical simulation. Also, we examined the log data of 2019 that was actually operated.

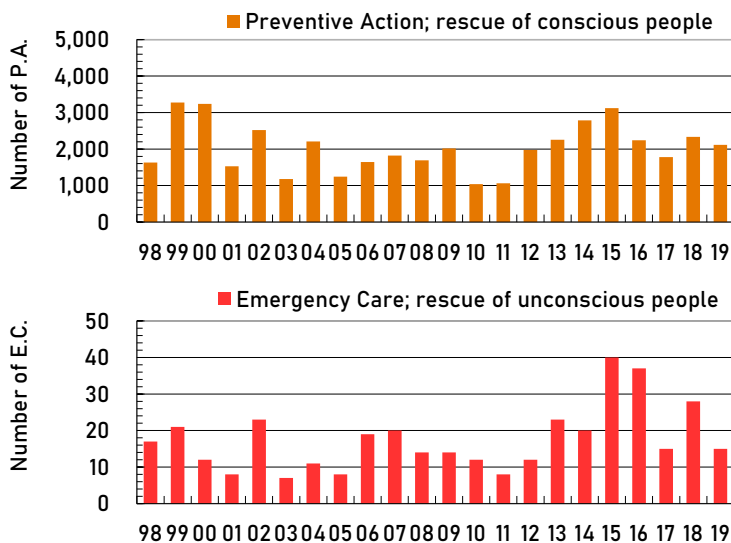


Figure 1. Number of Rescue from 1998 to 2019

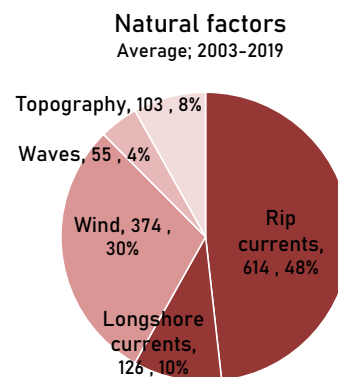


Figure 2. Outbreak factors of drowning accidents

2. Summary of Rip Current Detection System using AI and IoT

This technology automatically detects the rip current by the analysis of the AI using the surface image data of web cameras on the beach in real time. When rip currents are detected, an alert is automatically provided to digital signage and beach user's smartphone. It is effective for the risk awareness of the beach user. Furthermore, if the beach user enters the rip current area, lifeguards can take early action from the warning on their wearable device. Therefore, AI has 2 primary

functions which are rip currents detection and human detection (Fig. 3).

In order to realize this idea, we developed the system at the 1st study beach which was Onjuku beach in 2018. The study beach is located in near Tokyo, and faces the Pacific Ocean. The swimming area of the beach is about 300 m along the coast (Fig. 4), and the maximum number of visitors per day in recent years is about 10,000, and about 10 lifeguards are active. In addition, the average number of rescues on this beach is 145/year, and rip currents are over 50 % of the natural factors of drowning accidents, because flash rips are generated on this beach (Fig. 5).

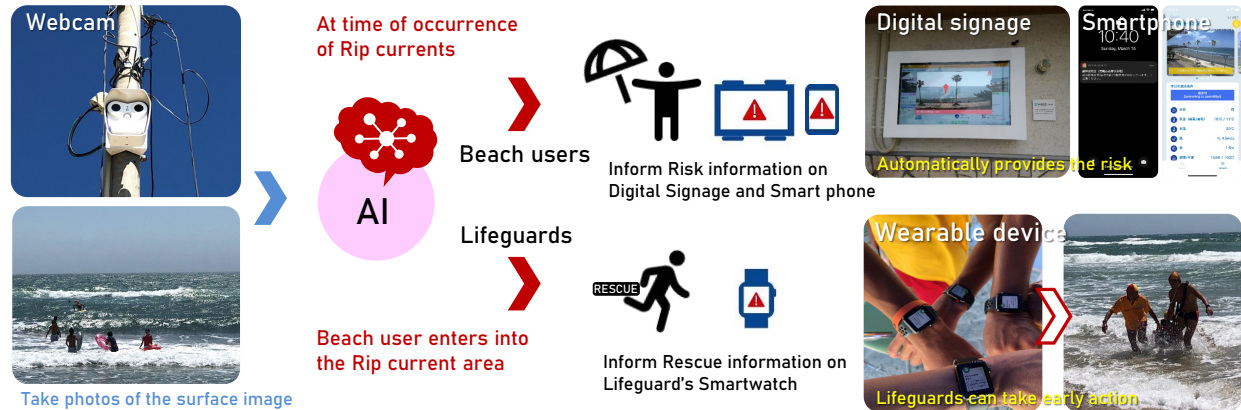


Figure 3. System overview diagram of rip current detection system using AI and IoT

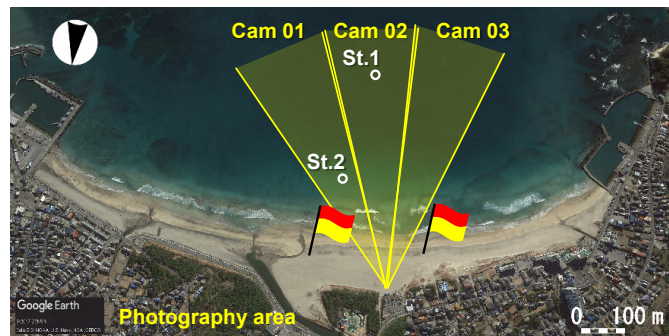


Figure 4. Study beach and photographing ranges



Figure 5. Example of rip current situation

The AI model for the rip current detection was made by thorough deep learning together with field observations on the study beach. In the deep learning, we collected 4 months of surface image data by 3 webcams which were set on the beach. The Image data was at a continuous rate of 3 per second. Next, we made 64,127 training data with different scale, horizontal rotation, hue, saturation, and lightness using the feature extraction from 100 annotation data of rip current image to make the AI model. The feature extraction was set by processing the differences of 3 consecutive images. Therefore, AI repeats the analysis at intervals of about 1 second. Figure 6 shows an example of image data of Cam01. Because the Cam01 was set diagonally in back of the shoreline and the height of the camera was low, above 4 m from the ground level, the rip current is shown at an oblique angle view in the image. However, the oblique angle view is limited to a rectangular shaped bounding box due to existing functions in the Annotation. For object detection algorithms, the *Tiny YOLO* (Redmon and Farhadi, 2017) was used for the rip current detection by AI, and the *YOLO v3* (Redmon and Farhadi, 2018) was used for the human detection. At the stage of making the AI model, the precision rate and the recall rate of the rip current detection by AI were 91.1 % and 86.6 % at the final point of the model evolution. Figure 7 shows an example of the result, a blue area of detection by AI coincides well with a red area of judgement by expert lifeguard. Similarly, we could get a good result for human entrance. The results of precision and recall were 96.5 % and 91.5 % respectively.

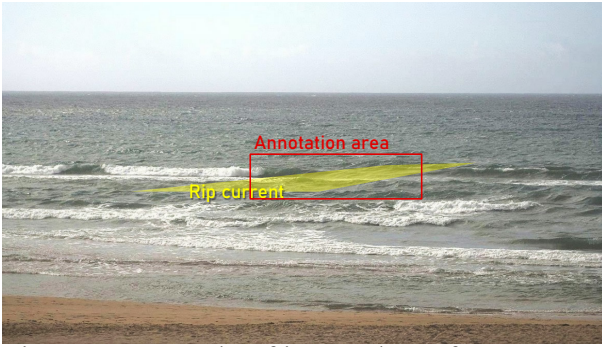


Figure 6. Example of image data of Cam 01

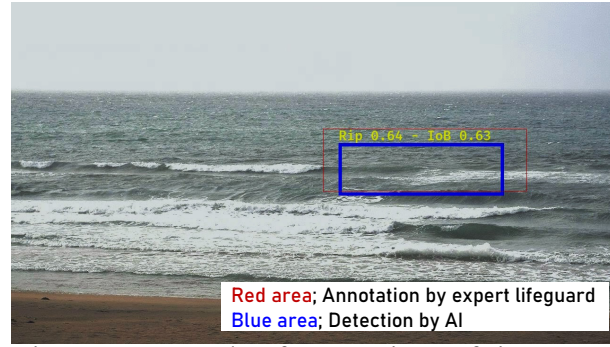


Figure 7. Example of comparison of rip current detection area by annotation and AI

3. Method of Verification of Rip current detection by AI

The system was operated as a trial on the study beach on December 2018. Figure 8 shows a result of incidence of rip currents every 20 minutes by AI detection for image of Cam 01 during the verification period between 9 and 25 on Dec. 2018. For example, the incidence of rip current detection was 65 % on 9 Dec., this means that rip currents were detected in 2,340 of 3,600 photos which were taken during the 20 min. In order to verified the accuracy of the rip current detection by AI, we investigated the accuracy for 49 cases with the incidence of 10 % or more and 165 cases with the incidence of 0 % which means a no rip current situation by a field measurement, an image analysis and a numerical simulation. We actually visually confirmed the presence or absence of rip currents in the images of each case, but used these methods as an objective evaluation. Figure 9 shows an example of the image of rip current detection by AI.

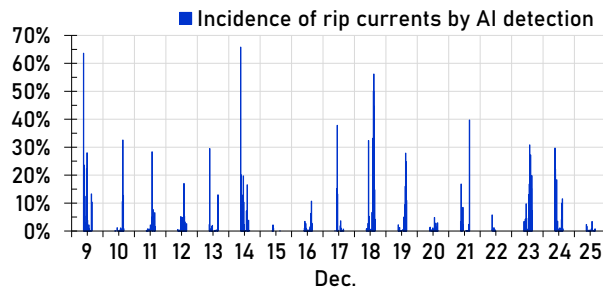


Figure 8. Incidence of rip currents on every 20 minutes by AI detection for Cam 01



Figure 9. Example of the image of rip current detection by AI (15:17, 19 December 2018)

In the field measurement, we set 2 supersonic wave gages at 2 and 7 m depth in the photography area of web cams. The wave gage of the St. 2 should have been set in shallow water to measure nearshore currents, but it was set at a depth of 2 m to avoid contact with surfers (Fig. 4, 10). Figure 11 shows the waves at St.2 during the observation period. The maximum significant wave was $H_{1/3} = 1.67$ m and $T_{1/3} = 6.43$ s at 18:40 on 19 December, and the number of waves exceeding $H_{1/3} = 1$ m was large. The energy mean wave during this period was $H = 0.59$ m and $T = 7.23$ s, and there were relatively calm conditions where it was possible to swim in the sea on the Onjuku beach facing the Pacific Ocean. Also, we carried out the rip currents survey using color dye during this period. The rip current was confirmed around 10:00 on 10 December as shown in Figure 12. Figure 13 shows the results of waves and currents during color dye survey at St. 2. The rip current directions from 135° to 225° were observed between 9:40 and 10:20. In the verification, we confirmed the rip current direction was observed at St.2 at the time of the rip current detection by AI.

In the image analysis, we applied this method which was proposed to observe water depth in

the surf zone, and the formation of a bar and trough by Lippmann and Holman (1989). Figure 14 shows an example of the result which was made at an averaged image of approximately 550 images every 5 minutes using image data of Cam 01. The rip current can be confirmed in the dark colored area with an oblique angle (a yellow dotted line of Fig. 14(a)), because the waves are hard to break in the rip current area. However, the dark colored area cannot be confirmed in the no rip current situation (Fig. 14(b)). Therefore, if the averaged image has the dark colored area that crosses the surf zone, we evaluated it as "rip current occurred". On the other hand, when there was not any dark colored area and the color was uniform, we evaluated it as "no rip current occurred".

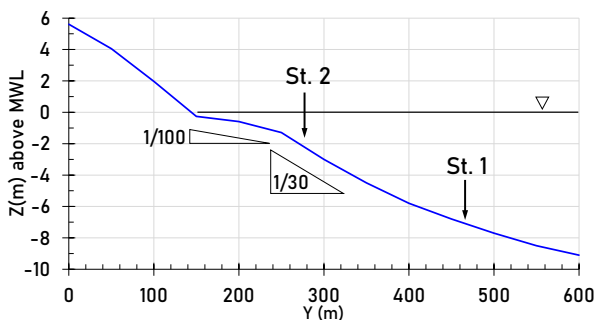


Figure 10. Longitudinal profile and position of wave gages

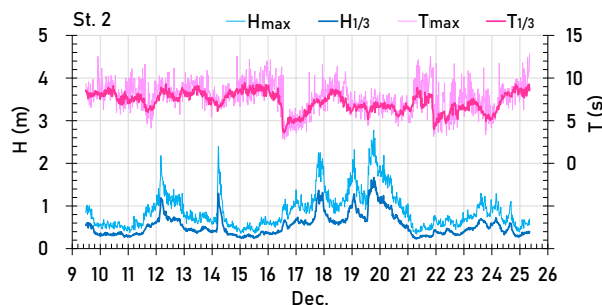


Figure 11. Field measurement results of waves at St. 2

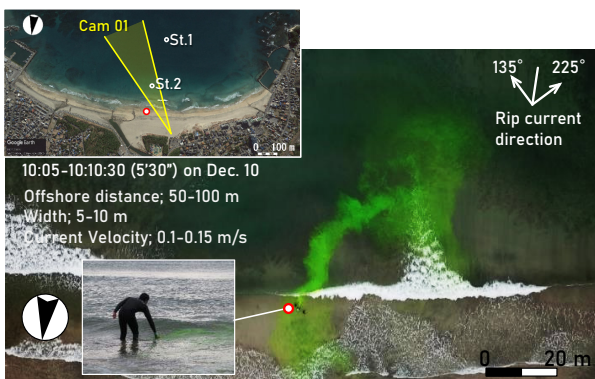


Figure 12. Situation of color dye survey

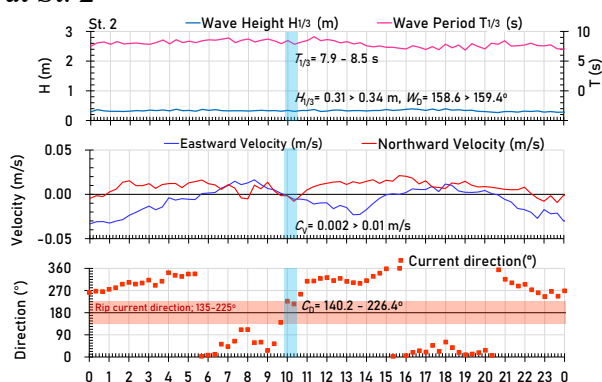
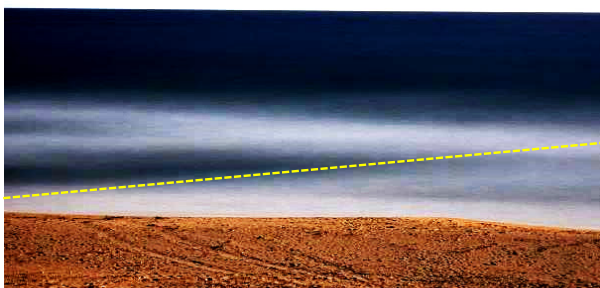


Figure 13. Field measurement results of waves and currents at St. 2 on 10 December



(a) 15:10-15:15, 19 December 2018 (case 32) (b) 15:40-15:45, 21 December 2018 (case 36)
 Figure 14. Example of the result of Image analysis in case 32 and 36

In the numerical simulation, the parabolic approximation to the elliptic mild-slope equation was used for a calculation of wave field, and the two-dimensional horizontal flow equations was used for a calculation of nearshore current (DHI, 2017). For the wave conditions, the observed

data of St.1 corresponding to each case were used, and for the tide conditions, the observed tide level of the Mera observatory of the Japan Meteorological Agency was used. Table 1 shows the calculation conditions. A validity of the calculation was confirmed by reproducing the occurrence of rip current within the same area of the color dye survey. Figure 15 shows the reproduction calculation result, the rip currents can be confirmed in the color dye survey area. Figure 16 is an example of the calculation results, in case of occurrence of rip currents, the rip currents can be confirmed in the photographing range of Cam 01. Even though the rip current was detected by AI in this case, rip currents were not calculated in Figure 17. Therefore, if the rip currents were calculated in the photographing range of Cam 01 as in Fig. 16, we evaluated it as "rip current occurred". On the other hand, in case of the no calculated rip currents as in Fig. 17, we evaluated it as "no rip current occurred".

In addition, the system using the developed AI model was actually operated on the study beach during summer from 2019. Thus, we examined the log data of 2019, we especially noticed the actual rescue cases. The log data records information for identifying the rip current and human detection time and the detection area such as the *XY* coordinates of the base point, width, and length.

Table 1 Calculation conditions

Area	Onjyuku Beach (2.4 km×1.2 km)
Topography	Observed at 2017
Case	Reproduction; Color dye survey (9:40-10:40, 10 Dec. 2018) Prediction; 46 cases of Rip current detection of 10% or more by AI 156 cases of No rip current detection by AI
Waves	Measured value at St.1 Reproduction; $H=0.34$ m, $T=8.47$ s, $W_D=154.4^\circ$ Prediction; Measured value for each case
Tide	Measured value at Mera observatory Reproduction; T.P.+0.24 m Prediction; Measured value for each case
Mesh size	$\Delta x = \Delta y = 2.5$ m
Wave field	Parabolic approximation to the elliptic mild-slope equation $\gamma_1=1, \gamma_2=0.8, K_n=0.002$
Nearshore current	two-dimensional horizontal flow equations $\varepsilon = 0.0, n = 0.031, \Delta t = 0.5$ s, 600 steps

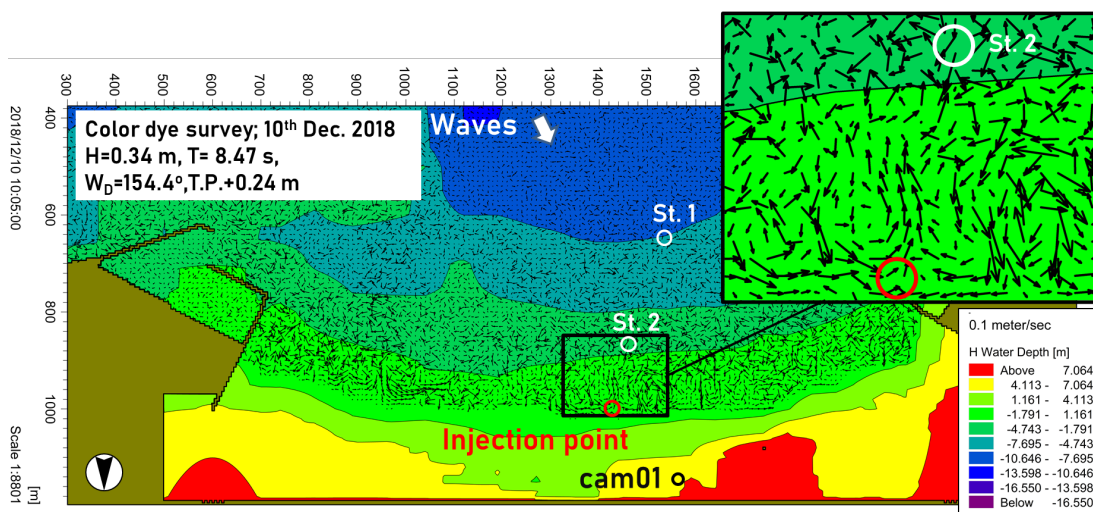


Figure 15. Reproduction calculation result for the color dye survey at 10:05 on 10 December

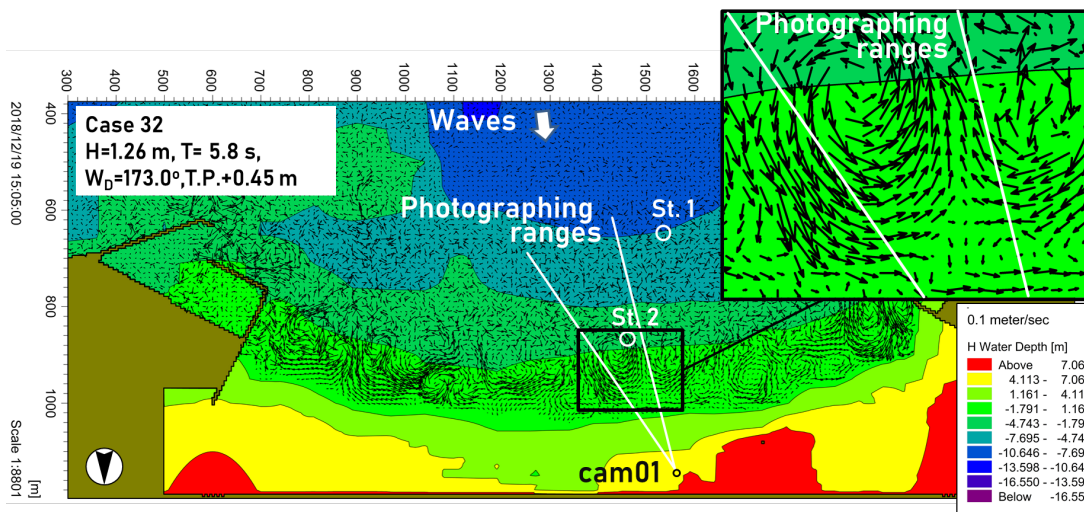


Figure 16. Example of the calculation result in case 32 of 28% of rip current detection by AI at 15:00-15:20 on 19 December 2018

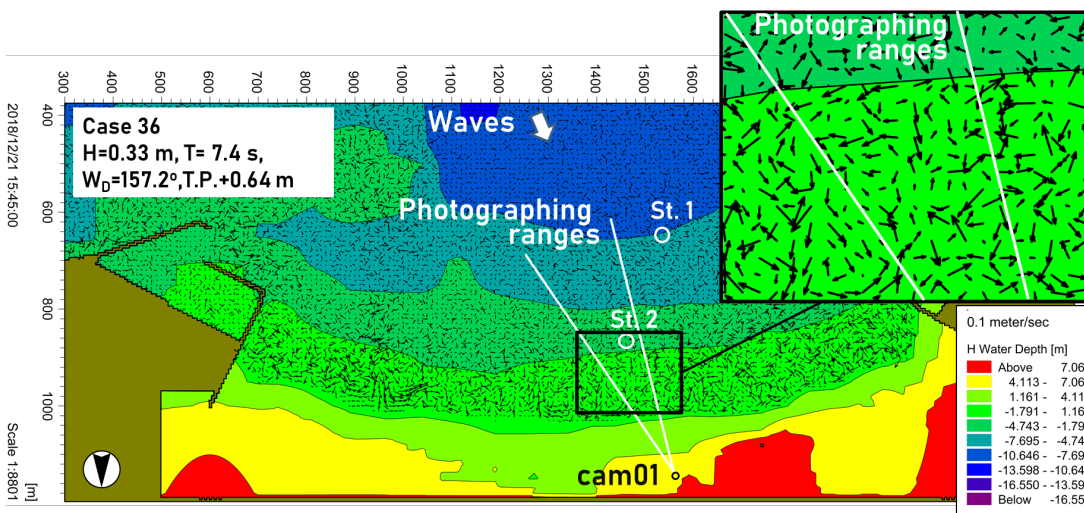


Figure 17. Example of the calculation result in case 36 of 39.7% of rip current detection by AI at 15:40-16:00 on 21 December 2018

4. Result

Table 2 shows verification results of the rip current detection of the 49 cases. Only 2 cases were able to confirm rip currents using all methods. 38 cases clearly had confirmed the dark colored area, and 5 cases had confirmed the dark colored area with part of the image in the image analysis. 31 cases had calculated predominant rip currents in the photographing range of Cam 01 in the numerical simulation, and 5 cases had calculated rip currents in a part of the photographing range. The accuracy rate of 88 % (43/49 cases) for the image analysis and 78 % (36/46 cases) for the numerical simulation respectively were confirmed during the observation period. However, the rip current direction was not observed in most cases by the field measurement. As for the reason, St. 2 was located offshore from the breaking zone during the observation period except during times with high waves. Also, it may have been difficult to observe a changing rip current in only one spot.

In the 165 cases in the no rip current situation, AI did not detect rip currents, but the occurrence of rip currents was confirmed in some cases as show in Figure 18 and 19. As a result, 95 cases had

not confirmed the rip currents, except for 9 cases that could not be confirmed due to the backlight in the image analysis. 149 cases had not calculated the rip currents in the photographing range of Cam 01 in the numerical simulation. The accuracy rate of 61 % (95/156 cases) for the image analysis and 90 % (149/165 cases) for the numerical simulation respectively were confirmed. This study has made it clear that the rip currents detection by AI was generally correct, but not all rip currents could be detected.

Table 2 Verification results of rip currents detection of 10 % or more by AI

Case	m/d h:m-h:m	Wave conditions (St.1)			Incidence of Rip current by AI (%)	Verification results		
		$H_{1/3}$ (m)	$T_{1/3}$ (s)	W_D (°)		Field measurement (St. 2)	Image analysis	Numerical simulation
1	12/9 9:00-9:20	—	—	—	63.6	—* ¹	Confirmed	—* ³
2	12/9 9:20-9:40	—	—	—	23.6	—* ¹	Confirmed	—* ³
3	12/9 10:00-10:20	—	—	—	12.5	—* ¹	Confirmed	—* ³
4	12/9 11:20-11:40	0.54	8.1	164.6	22.3	—* ¹	Confirmed	Calculated
5	12/9 11:40-12:00	0.53	8.1	165.4	28.0	Not	Confirmed	Calculated
6	12/9 15:00-15:20	0.58	8.3	164.0	13.3	Not	Not	Not
7	12/9 15:20-15:40	0.54	7.9	162.2	10.4	Not	Confirmed	Calculated
8	12/10 14:40-15:00	0.35	7.3	153.1	10.6	Not	Confirmed	Not
9	12/10 15:00-15:20	0.37	7.6	150.4	32.6	Not	Not	Not
10	12/10 15:20-15:40	0.39	7.5	151.1	12.7	Not	Confirmed* ²	Calculated
11	12/11 13:20-13:40	0.46	7.7	150.3	28.4	Not	Confirmed	Calculated
12	12/12 13:40-14:00	0.78	8.0	154.8	17.0	Not	Confirmed	Calculated
13	12/13 9:20-9:40	0.38	7.9	153.1	29.5	Not	Confirmed	Calculated
14	12/13 15:40-16:00	0.46	8.0	151.8	13.0	Not	Confirmed	Calculated* ⁴
15	12/14 9:00-9:20	0.66	6.9	164.2	65.8	Not	Confirmed	Calculated* ⁴
16	12/14 9:20-9:40	0.56	7.1	162.1	20.1	Not	Confirmed	Calculated
17	12/14 10:00-10:20	0.58	7.5	163.7	12.9	Not	Not	Calculated
18	12/14 11:00-11:20	0.43	7.5	162.7	19.7	Not	Not	Calculated* ⁴
19	12/14 11:20-11:40	0.39	7.1	167.0	10.3	Not	Confirmed	Calculated* ⁴
20	12/14 13:40-14:00	0.35	7.9	162.1	16.5	Not	Confirmed	Not
21	12/16 15:00-15:20	0.72	3.9	159.6	10.7	Not	Confirmed	Calculated
22	12/17 10:20-10:40	0.65	6.0	159.0	15.1	Not	Confirmed	Calculated
23	12/17 10:40-11:00	0.65	6.2	157.6	37.8	Not	Confirmed	Calculated
24	12/17 11:00-11:20	0.65	6.1	158.7	13.2	Not	Confirmed	Calculated
25	12/18 10:40-11:00	0.66	8.4	161.8	32.4	Not	Confirmed	Calculated
26	12/18 14:00-14:20	0.59	7.7	165.2	33.2	Not	Confirmed	Calculated
27	12/18 14:20-14:40	0.62	7.5	165.5	50.1	Observed	Confirmed	Calculated
28	12/18 14:40-15:00	0.68	7.6	164.0	56.2	Observed	Confirmed	Calculated
29	12/18 15:00-15:20	0.64	7.3	166.3	44.6	Not	Confirmed	Calculated
30	12/18 15:20-15:40	0.64	7.5	166.4	14.8	Not	Confirmed	Calculated
31	12/19 14:40-15:00	1.28	5.6	174.1	16.0	Not	Confirmed	Calculated
32	12/19 15:00-15:20	1.26	5.8	173.0	27.9	Not	Confirmed	Calculated
33	12/19 15:20-15:40	1.24	6.1	173.5	24.8	Not	Confirmed	Calculated
34	12/19 15:40-16:00	1.34	6.3	173.8	11.0	Not	Confirmed	Calculated
35	12/21 9:20-9:40	0.27	7.8	160.9	16.8	Not	Not	Calculated* ⁴
36	12/21 15:40-16:00	0.33	7.4	157.2	39.7	Not	Not	Not
37	12/23 13:00-13:20	0.68	6.6	154.4	13.0	Not	Confirmed	Calculated
38	12/23 13:20-13:40	0.72	6.6	153.8	16.8	Not	Confirmed	Calculated
39	12/23 13:40-14:00	0.77	6.8	152.8	30.8	Not	Confirmed	Not
40	12/23 14:00-14:20	0.74	6.4	152.3	11.1	Not	Confirmed	Not
41	12/23 14:20-14:40	0.73	6.2	150.7	27.2	Not	Confirmed	Not

Case	m/d h:m-h:m	Wave conditions (St.1)			Incidence of Rip current by AI (%)	Verification results		
		$H_{1/3}$ (m)	$T_{1/3}$ (s)	W_D (°)		Field measurement (St. 2)	Image analysis	Numerical simulation
42	12/23 14:40-15:00	0.71	6.3	157.4	13.8	Not	Confirmed	Not
43	12/23 15:00-15:20	0.77	6.3	156.2	15.2	Not	Confirmed	Calculated
44	12/23 15:20-15:40	0.72	6.3	155.8	19.8	Not	Confirmed	Not
45	12/24 9:00-9:20	0.49	7.7	163.4	29.7	Not	Confirmed	Calculated
46	12/24 9:20-9:40	0.50	7.5	164.7	22.2	Not	Confirmed* ²	Calculated
47	12/24 10:20-10:40	0.40	7.4	164.5	18.3	Not	Confirmed* ²	Calculated
48	12/24 14:20-14:40	0.49	8.3	165.6	10.0	Not	Confirmed* ²	Calculated
49	12/24 14:40-15:00	0.54	8.1	167.0	11.5	Not	Confirmed* ²	Calculated

*¹ No data for St. 2 (before observation started of St. 2)
 *² Difficult to confirm due to backlight, but a dark colored area was confirmed in a part of the image.
 *³ No data for St. 1 (before observation started of St. 1)
 *⁴ Predominant rip currents were not calculated, but the rip currents in a part of the photographing range of Cam 01 were calculated.



Figure 18. Example of the image analysis result of no rip current detection by AI at 11:40-11:45 on 19 December 2018

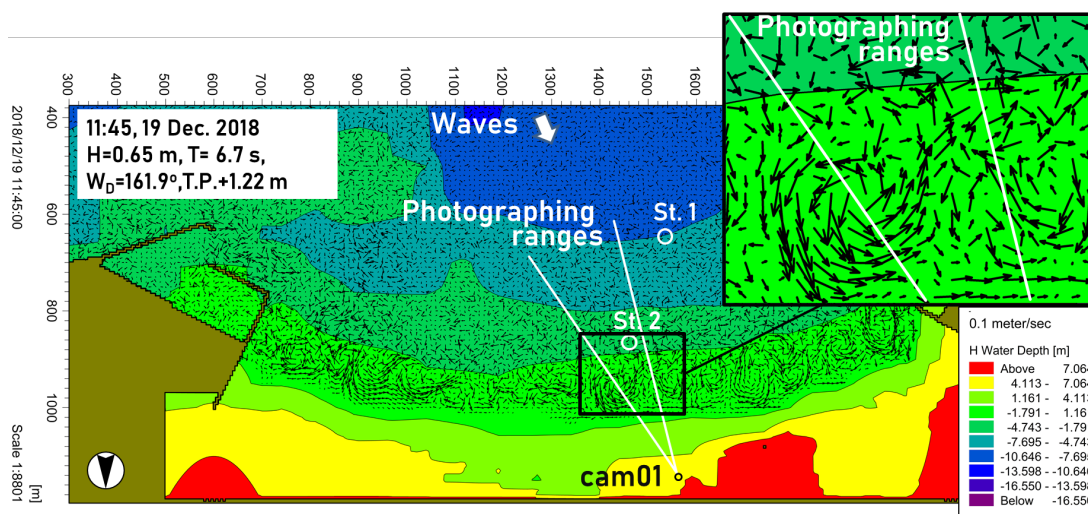
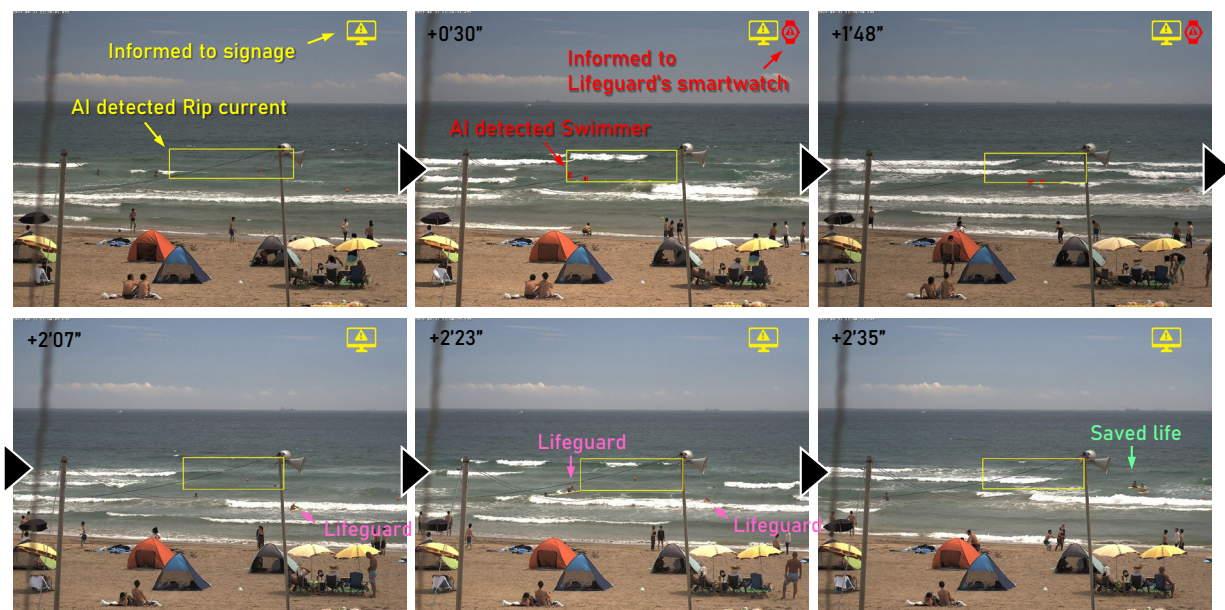
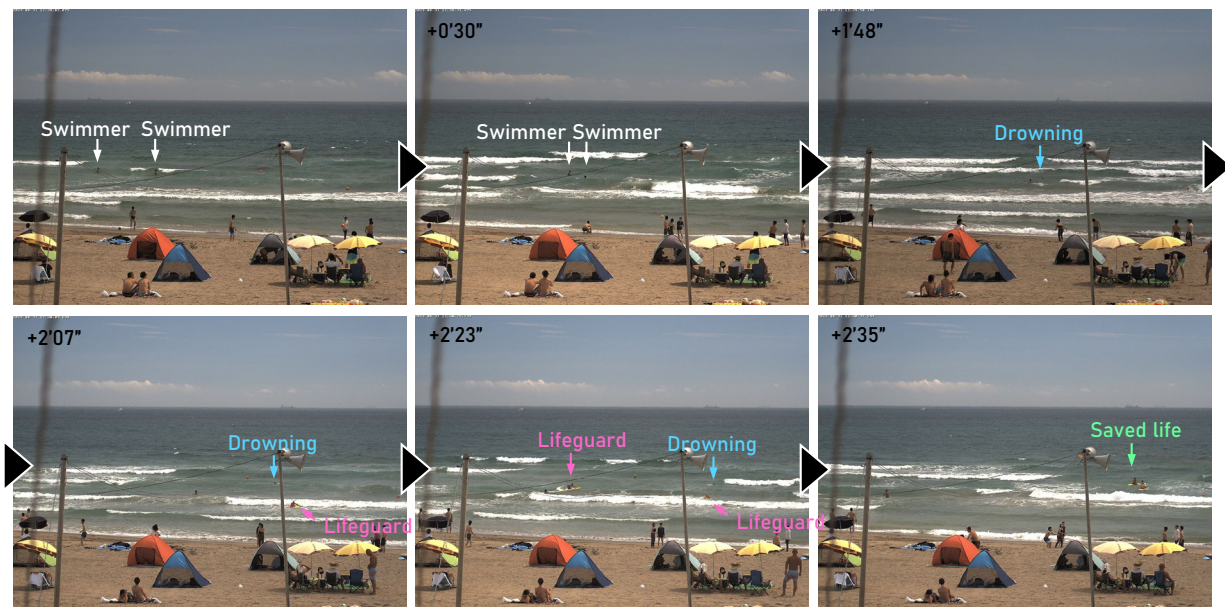


Figure 19. Example of the calculation result of no rip current detection by AI at 11:40-12:00 on 19 December 2018

The system using the developed AI model was actually operated on the study beach during summer from 2019. As a result of the hearing surveys with lifeguards ($n = 20$) in 2019, the rip current detection of 65 % and the human detection of 80 % were mostly correct. The total number

of rip current alerts by the system were 2,425 for a total of 51 days from July to August 2019. In fact, some swimmers were rescued by lifeguards under the system. Figure 20 shows an example of a rip current accident. It can be confirmed that one swimmer was drowning in the rip current area. Figure 21 shows the detection areas by the analysis of the system log data on the images at same time as Fig. 20. It was confirmed AI could detect rip currents and human entrance into rip current areas. Also, the detected rip current areas mostly accorded with actual rip current areas which shift due to wave conditions. In this rip current accident, although the swimmer was near drowning, lifeguards could take early action by receiving the information quickly from the system to their smartwatches. The life of the swimmer was saved by approximately 50 seconds. As in this example, some swimmers were rescued by lifeguards under the system in 2019.



5. Conclusion

In this study, we verified the accuracy of the AI function which detects the rip currents using 3 methods. As a result, it was confirmed that the accuracy of rip current generation by AI was 88 % in the image analysis and 78 % in the numerical simulation, and the accuracy of no rip current generation by AI was 61 % and 90 % respectively. Therefore, it was clear that AI could not detect all rip currents. However, considering the actual operation results, it is generally beneficial and it is thought that it can contribute to the drowning prevention.

The system has actually been operated at 3 beaches up to 2021. The AI model eventually must be able to detect all rip currents. Also, it should be created accordingly on individual beaches. It has not been a general-purpose technology yet. We think these issues can be solved by it being applied to many beaches.

Acknowledgements

This study was funded by the Ministry of Internal Affairs and Communications of Japan in 2018. It was also funded by the Nippon Foundation and the Japan Lifesaving Association in 2019 and 2020.

References

- Ishikawa, T., Komine, T., Aoki, S., and Okabe, T. 2014. "Characteristics of Rip Current Drowning on the Shores of Japan." *Journal of Coastal Research*, 72(10072), 44-49.
- Brighton, B., Sherker, S., Brander, R., Thompson, M., & Bradstreet, A. 2013. "Rip current related drowning deaths and rescues in Australia 2004-2011." *Natural Hazards and Earth System Sciences*, 13, 1069-1075.
- Redmon, J. and Farhadi, A. 2017. "Yolo9000: Better, faster, stronger." In *Computer Vision and Pattern Recognition (CVPR), IEEE Conference*, 6517-6525.
- Redmon, J. and Farhadi, A. 2018. "Yolov3: An incremental improvement." *arXiv*, 1-6.
- Lippmann, T. C. and Holman, R. A. 1989. "Quantification of Sand Bar Morphology - A Video Technique Based on Wave Dissipation." *JGR*, Vol. 94, 995-1011.
- DHI. 2017. *MIKE21 Parabolic Mild-Slope Wave Module Scientific Documentation*.
- DHI. 2017. *MIKE21 Flow Model & Flood Screening Tool Hydrodynamic Module Scientific Documentation*.